

---

---

**Measurement of fluid flow by means  
of pressure differential devices —  
Guidelines on the effect of departure  
from the specifications and operating  
conditions given in ISO 5167**

*Mesurage du débit des fluides au moyen d'appareils déprimogènes —  
Lignes directrices relatives aux effets des écarts par rapport aux  
spécifications et aux conditions d'utilisation données dans l'ISO 5167*

STANDARDSISO.COM : Click to view the full PDF of ISO/TR 12767:2023



STANDARDSISO.COM : Click to view the full PDF of ISO/TR 12767:2023



**COPYRIGHT PROTECTED DOCUMENT**

© ISO 2023

All rights reserved. Unless otherwise specified, or required in the context of its implementation, no part of this publication may be reproduced or utilized otherwise in any form or by any means, electronic or mechanical, including photocopying, or posting on the internet or an intranet, without prior written permission. Permission can be requested from either ISO at the address below or ISO's member body in the country of the requester.

ISO copyright office  
CP 401 • Ch. de Blandonnet 8  
CH-1214 Vernier, Geneva  
Phone: +41 22 749 01 11  
Email: [copyright@iso.org](mailto:copyright@iso.org)  
Website: [www.iso.org](http://www.iso.org)

Published in Switzerland

# Contents

	Page
Foreword.....	v
Introduction.....	vi
<b>1 Scope.....</b>	<b>1</b>
<b>2 Normative references.....</b>	<b>1</b>
<b>3 Terms and definitions.....</b>	<b>1</b>
<b>4 Symbols.....</b>	<b>2</b>
<b>5 Effect of errors on flowrate calculations.....</b>	<b>3</b>
5.1 General.....	3
5.2 Quantifiable effects.....	3
<b>6 Effects of deviations in construction.....</b>	<b>3</b>
6.1 Orifice-plate edge sharpness.....	3
6.2 Thickness of orifice edge.....	4
6.3 Condition of upstream and downstream faces of orifice plate.....	5
6.4 Position of pressure tapplings for an orifice.....	6
6.4.1 General.....	6
6.4.2 Calculation of discharge coefficient.....	6
6.4.3 Estimation of additional uncertainty.....	6
6.4.4 Example.....	6
6.5 Condition of pressure tapplings.....	7
<b>7 Effects of pipeline near the meter.....</b>	<b>7</b>
7.1 Pipe diameter.....	7
7.2 Steps and taper sections.....	7
7.3 Diameter of carrier ring.....	8
7.4 Undersize joint rings.....	11
7.5 Protruding welds.....	11
7.6 Eccentricity.....	11
<b>8 Effects of pipe layout.....</b>	<b>13</b>
8.1 General.....	13
8.2 Discharge coefficient compensation.....	14
8.2.1 Corrections.....	14
8.2.2 Additional uncertainty.....	15
8.3 Pressure tapplings.....	16
8.4 Devices for improving flow conditions.....	16
<b>9 Operational deviations.....</b>	<b>16</b>
9.1 General.....	16
9.2 Deformation of an orifice plate.....	17
9.2.1 General.....	17
9.2.2 Elastic deformation.....	17
9.2.3 Plastic deformation.....	17
9.3 Deposition on the upstream face of an orifice plate.....	18
9.4 Deposition in the meter tube.....	22
9.5 Orifice-plate edge sharpness.....	23
9.5.1 Deterioration.....	23
9.5.2 Plate reversal.....	23
9.6 Deposition and increase of surface roughness in Venturi tubes.....	24
9.6.1 General.....	24
9.6.2 Deposition.....	24
9.6.3 Surface roughness.....	24
<b>10 Pipe roughness.....</b>	<b>25</b>
10.1 General.....	25

10.2	Upstream pipe.....	26
10.3	Downstream pipe.....	30
10.4	Reduction of roughness effects .....	30
10.5	Maintenance.....	30
<b>Bibliography .....</b>		<b>32</b>

STANDARDSISO.COM : Click to view the full PDF of ISO/TR 12767:2023

## Foreword

ISO (the International Organization for Standardization) is a worldwide federation of national standards bodies (ISO member bodies). The work of preparing International Standards is normally carried out through ISO technical committees. Each member body interested in a subject for which a technical committee has been established has the right to be represented on that committee. International organizations, governmental and non-governmental, in liaison with ISO, also take part in the work. ISO collaborates closely with the International Electrotechnical Commission (IEC) on all matters of electrotechnical standardization.

The procedures used to develop this document and those intended for its further maintenance are described in the ISO/IEC Directives, Part 1. In particular, the different approval criteria needed for the different types of ISO document should be noted. This document was drafted in accordance with the editorial rules of the ISO/IEC Directives, Part 2 (see [www.iso.org/directives](http://www.iso.org/directives)).

ISO draws attention to the possibility that the implementation of this document may involve the use of (a) patent(s). ISO takes no position concerning the evidence, validity or applicability of any claimed patent rights in respect thereof. As of the date of publication of this document, ISO had not received notice of (a) patent(s) which may be required to implement this document. However, implementers are cautioned that this may not represent the latest information, which may be obtained from the patent database available at [www.iso.org/patents](http://www.iso.org/patents). ISO shall not be held responsible for identifying any or all such patent rights.

Any trade name used in this document is information given for the convenience of users and does not constitute an endorsement.

For an explanation of the voluntary nature of standards, the meaning of ISO specific terms and expressions related to conformity assessment, as well as information about ISO's adherence to the World Trade Organization (WTO) principles in the Technical Barriers to Trade (TBT), see [www.iso.org/iso/foreword.html](http://www.iso.org/iso/foreword.html).

This document was prepared by Technical Committee ISO/TC 30, *Measurement of fluid flow in closed conduits*, Subcommittee SC 2, *Pressure differential devices*.

This third edition cancels and replaces the second edition (ISO/TR 12767:2007), which has been technically revised.

The main changes are as follows:

- editorial changes throughout the document.

Any feedback or questions on this document should be directed to the user's national standards body. A complete listing of these bodies can be found at [www.iso.org/members.html](http://www.iso.org/members.html).

## Introduction

ISO 5167 series specifies methods for flowrate measurement using pressure differential devices. Adherence to ISO 5167 series results in flowrate measurements whose uncertainty lies within specified limits. If, however, a flow-metering installation departs, for whatever reason, from the conditions specified in ISO 5167 series, the specified limits of uncertainty might not be achieved. Many metering installations exist where these conditions either have not been or cannot be met. In these circumstances, it is usually not possible to evaluate the precise effect of any such deviations. However, a considerable amount of data exists which can be used to give a general indication of the effect of non-conformity to ISO 5167 series and it is presented in this document as a guideline to users of flow-metering equipment.

STANDARDSISO.COM : Click to view the full PDF of ISO/TR 12767:2023

# Measurement of fluid flow by means of pressure differential devices — Guidelines on the effect of departure from the specifications and operating conditions given in ISO 5167

## 1 Scope

This document provides guidance on estimating the flowrate when using pressure differential devices constructed or operated outside the scope of ISO 5167 series.

Additional tolerances or corrections cannot necessarily compensate for the effects of deviating from ISO 5167 series. The information is given, in the first place, to indicate the degree of care necessary in the manufacture, installation and maintenance of pressure differential devices by describing some of the effects of non-conformity to the requirements; and in the second place, to permit those users who cannot comply fully with the requirements to assess, however roughly, the magnitude and direction of the resulting error in flowrate.

Each variation dealt with is treated as though it were the only one present. Where more than one is known to exist, there might be unpredictable interactions and care has to be taken when combining the assessment of these errors. If there is a significant number of errors, means of eliminating some of them have to be considered. The variations included in this document are by no means complete and relate largely to examples with orifice plates. An example with Venturi tubes has been placed at the end of its section. This document does not apply to cone meters or wedge meters. There are, no doubt, many similar examples of installations not conforming to ISO 5167 series for which no comparable data have been published. Such additional information from users, manufacturers and any others can be taken into account in future revisions of this document.

## 2 Normative references

The following documents are referred to in the text in such a way that some or all of their content constitutes requirements of this document. For dated references, only the edition cited applies. For undated references, the latest edition of the referenced document (including any amendments) applies.

ISO 5167-1, *Measurement of fluid flow by means of pressure differential devices inserted in circular cross-section conduits running full — Part 1: General principles and requirements*

## 3 Terms and definitions

For the purposes of this document, the terms and definitions given in ISO 5167-1 and the following apply.

ISO and IEC maintain terminology databases for use in standardization at the following addresses:

- ISO Online browsing platform: available at <https://www.iso.org/obp>
- IEC Electropedia: available at <https://www.electropedia.org/>

### 3.1

#### square edge

angular relationship between the orifice bore of the flow-measurement device and the upstream face, when the angle between them is  $90^\circ \pm 0,3^\circ$

## 3.2

**sharpness**

radius of the edge between the orifice bore of the flow-measurement device and the upstream face

Note 1 to entry: The upstream edge of the orifice bore is considered to be sharp when its radius is not greater than  $0,000\ 4d$ , where  $d$  is the diameter of the orifice bore.

## 4 Symbols

For the purposes of this document, the symbols given in [Table 1](#) apply.

Table 1 — Symbols and units

Symbol	Quantity represented	Dimension M: mass L: length T: time	SI unit
$c$	Percentage change in discharge coefficient $[= 100(\Delta C / C)]$	dimensionless	
$C$	Discharge coefficient	dimensionless	
$C_c$	Contraction coefficient	dimensionless	
$d$	Diameter of orifice or throat of primary device under working conditions	L	m
$D$	Upstream internal pipe diameter under working conditions	L	m
$D_1$	Carrier ring diameter	L	m
$D_2$	Orifice-plate support diameter	L	m
$e$	Orifice thickness	L	m
$E$	Orifice-plate thickness	L	m
$k$	Uniform equivalent roughness	L	m
$L_1$	Distance of upstream pressure tapping from upstream face of plate divided by pipe bore, $D$	dimensionless	
$L'_2$	Distance of downstream pressure tapping from downstream face of plate divided by pipe bore, $D$	dimensionless	
$q_m$	Mass flow rate	$MT^{-1}$	kg/s
$r$	Orifice-plate edge radius	L	m
$Re_d$	Throat Reynolds number	dimensionless	
$Re_D$	Pipe Reynolds number	dimensionless	
$u$	Local axial velocity	$LT^{-1}$	m/s
$u_{CL}$	Centreline axial velocity	$LT^{-1}$	m/s
$U$	Mean axial velocity	$LT^{-1}$	m/s
$U'$	Relative expanded uncertainty	dimensionless	
$Y$	Modulus of elasticity of orifice-plate material	$ML^{-1}T^{-2}$	Pa
$\beta$	Diameter ratio, $(= d/D)$	dimensionless	
$\Delta p$	Differential pressure	$ML^{-1}T^{-2}$	Pa
$\Delta p_y$	Differential pressure required to reach orifice-plate yield stress	$ML^{-1}T^{-2}$	Pa
$\varepsilon$	Expansibility (expansion) factor	dimensionless	
$\lambda$	Friction factor	dimensionless	
$\rho$	Fluid density	$ML^{-3}$	kg/m <sup>3</sup>
$\rho_1$	Fluid density at the upstream pressure tapping	$ML^{-3}$	kg/m <sup>3</sup>
$\sigma_y$	Yield stress of orifice-plate material	$ML^{-1}T^{-2}$	Pa



## 5 Effect of errors on flowrate calculations

### 5.1 General

In this document, the effects of deviations from the conditions specified in ISO 5167 series are described in terms of changes in the discharge coefficient,  $\Delta C$ , of the meter. The discharge coefficient,  $C$ , of a pressure differential device is given by [Formula \(1\)](#):

$$C = \frac{4q_m \sqrt{(1 - \beta^4)}}{\varepsilon \pi d^2 \sqrt{(2\Delta p \rho_1)}} \quad (1)$$

The sharp edge of an orifice plate ensures separation of the flow and consequently contraction of the fluid stream to the vena contracta. Defining the contraction coefficient,  $C_c$ , as the ratio of the flow area to the geometric area the orifice produces  $C_c \approx 0,6$ , which mainly accounts for the discharge coefficient,  $C \approx 0,6$ .

The effect of change in the discharge coefficient is illustrated by the following example.

Consider an orifice plate with an unduly rounded edge. The result of this is to reduce the separation and increase  $C_c$  leading in turn to reduced velocities at the vena contracta. The observed differential pressure therefore decreases. From [Formula \(1\)](#), it can be seen that the discharge coefficient therefore increases. Alternatively, as  $C_c$  increases, so does  $C$ . If no correction is made for this change in  $C$ , the meter reading is less than the actual value.

It can therefore be concluded that

- a) an effect which causes an increase in discharge coefficient results in a flowrate reading lower than the actual value if the coefficient is not corrected,
- and conversely,
- b) an effect which causes a decrease in discharge coefficient results in a flowrate reading higher than the actual value if the coefficient is not corrected.

### 5.2 Quantifiable effects

When the user is aware of such effects and they can be quantified, the appropriate discharge coefficient can be used and the correct flowrate calculated. However, the precise quantification of these effects is difficult and so any flowrate calculated in such a manner is considered to have an increased uncertainty.

Except where otherwise stated, an additional uncertainty factor, equivalent to 100 % of the discharge coefficient correction, is added arithmetically to the relative expanded uncertainty of the discharge coefficient when estimating the overall uncertainty in the flowrate measurement.

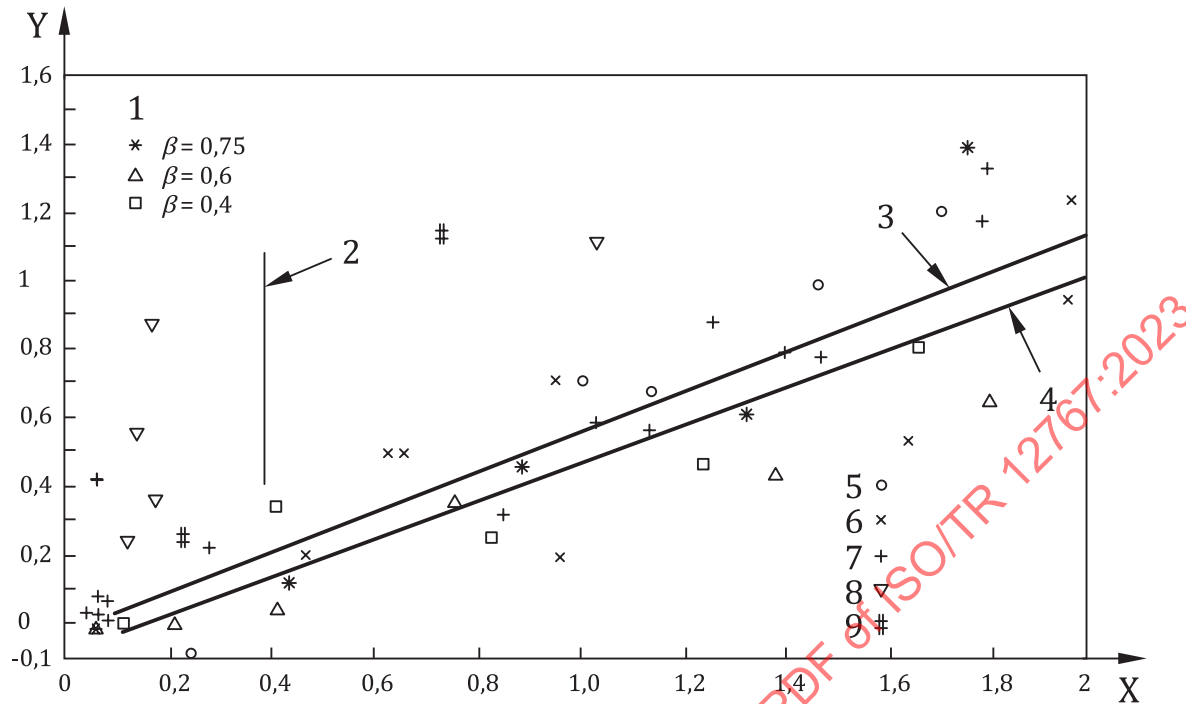
## 6 Effects of deviations in construction

### 6.1 Orifice-plate edge sharpness

Orifice plates that do not have the specified sharpness of the inlet edge (edge radius  $r \leq 0,000\ 4d$  in accordance with ISO 5167-2:2022, 5.1.7.2), have progressively increasing discharge coefficients as the edge radius increases. Tests have shown that the effect on the discharge coefficient,  $C$ , is to increase it by 0,5 % for  $r/d$  of 0,001, and by about 5 % for  $r/d$  of 0,01. This is an approximately linear relationship (see [Figure 1](#) and Reference [6]). These values apply particularly to  $Re_d$  values above 300 000 and for  $\beta$  values below 0,7, but they can be used as a general guide for other values.

Measurement techniques for edge radius are available, but in general it is better to improve the edge sharpness to the required value rather than to attempt to measure it and make appropriate corrections.

The effect of nicks in orifice plates has also been measured in Reference [6].



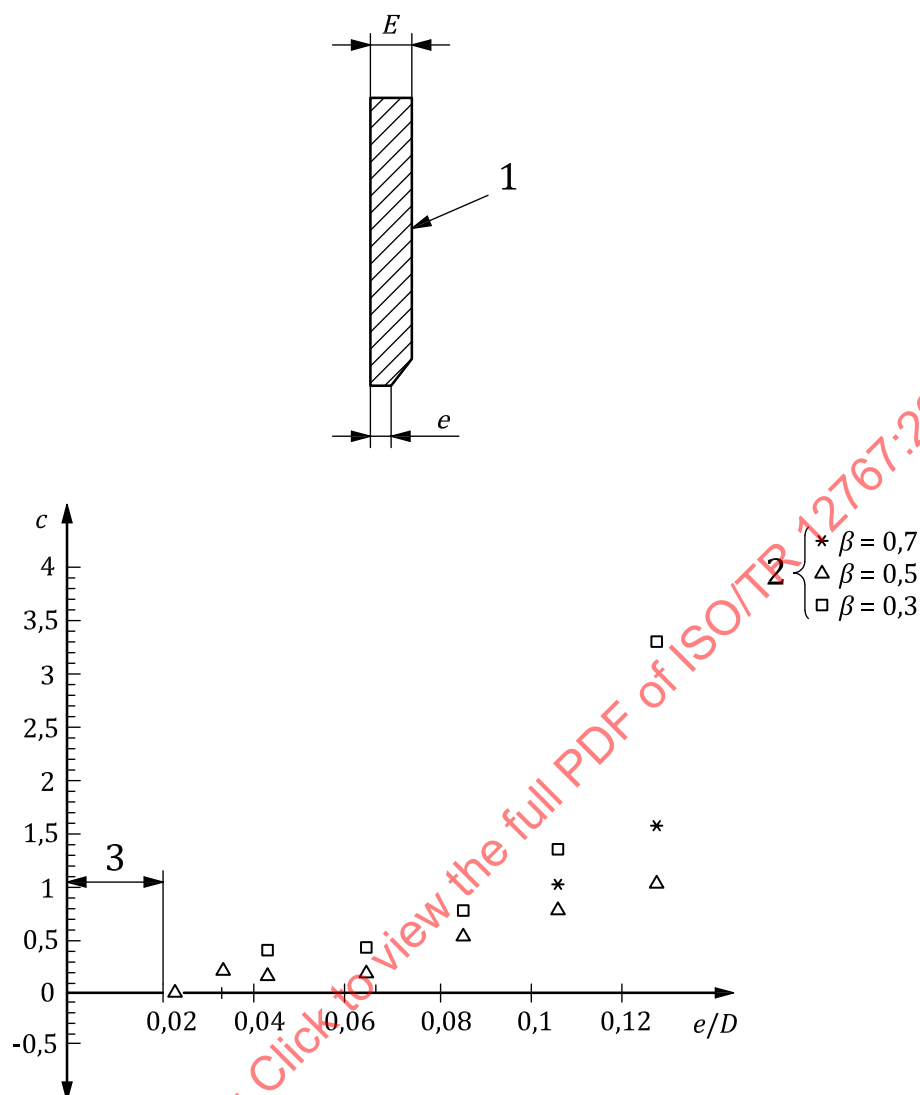
#### Key

- X radius ratio ( $r/d$ ) ( $\times 10^3$ )  
Y change in discharge coefficient (%)  
1 national engineering laboratory (NEL, UK) tests —  $D = 300$  mm  
2 ISO limit —  $r = 0,000\ 4d$   
3 others  
4 NEL  
5  $D = 50$  mm (Reference [59])  
6  $D = 100$  mm (Reference [59])  
7  $D = 150$  mm (Reference [37])  
8  $D = 75$  mm (Reference [60])  
9  $D = 100$  mm (Reference [61])

Figure 1 — Effect of edge radius on discharge coefficient

## 6.2 Thickness of orifice edge

For orifice plates, the increase in discharge coefficient due to excessive thickness of the orifice edge (see ISO 5167-2:2022, 5.1.5) can be appreciable. With a straight-bore orifice plate in a 150 mm pipe, the changes in discharge coefficient shown in Figure 2 were obtained (see Reference [7]). Additional data are shown in Reference [62].

**Key**

- 1 section of an orifice plate
- 2 symbol
- 3 limit of standard
- c change in discharge coefficient (%)
- e/D orifice thickness to upstream internal pipe diameter ratio

**Figure 2 — Change in discharge coefficient as a function of orifice thickness**

### 6.3 Condition of upstream and downstream faces of orifice plate

The upstream face of an orifice plate is flat and smooth. Excessive roughness leads to an increase in the discharge coefficient. Tests have indicated that a surface roughness of  $0,000\ 3d$  causes an increase in discharge coefficient of the order of 0,1 % (see Reference [34]). Since the requirement for edge sharpness is  $r \leq 0,000\ 4d$ , an increase in plate roughness makes it difficult to define the edge sharpness or to confirm that the sharp edge requirement has been met.

Local damage to the upstream face or edge of an orifice plate does not adversely affect the discharge coefficient, provided that the damage is kept as far away from the pressure tapping as possible (see Reference [6]). The discharge coefficient is much less sensitive to the surface condition of the downstream face of the plate (Reference [6]).

Large-scale lack of flatness, e.g. “dishing”, leads to flow-measurement errors. A “dishing” of 1 % in the direction of flow causes the reading to be below the actual value, i.e. an increase in  $C$  of about 0,2 % for  $\beta = 0,2$  and of about 0,1 % for  $\beta = 0,7$ . Distortion against the direction of flow also causes errors which could be either positive or negative depending on the amount of distortion.

## 6.4 Position of pressure tapplings for an orifice

### 6.4.1 General

Values of the orifice-plate discharge coefficient for the three standard tapping positions (corner, flange,  $D$  and  $D/2$ ) can be calculated using ISO 5167-2:2022, Formula (4) (see Reference [58]). Where the tapping positions fall outside the tolerances permitted in ISO 5167-2 for the three positions, the discharge coefficient is estimated as described in 6.4.2. An additional uncertainty factor is associated with the use of non-standard tapping positions.

### 6.4.2 Calculation of discharge coefficient

Calculate the actual values of  $L_1$  and  $L'_2$ . The discharge coefficient can be estimated only if  $L_1 \leq 1$  and  $L'_2 \leq 0,47$ .

Using the actual values of  $L_1$  and  $L'_2$  estimate the discharge coefficient using ISO 5167-2:2022, Formula (4).

### 6.4.3 Estimation of additional uncertainty

If tapplings lie between the flange and the corner tapplings, the additional uncertainty,  $\delta U'$ , expressed as a percentage, can be estimated from Formula (2):

$$\delta U' = 25 \left| \frac{C_F}{C_{CT}} - 1 \right| \quad (2)$$

where

$C_F$  is the discharge coefficient for flange tapplings;

$C_{CT}$  is the discharge coefficient for corner tapplings.

If tapplings lie between the  $D$  and  $D/2$  tapplings and the flange tapplings, the additional uncertainty,  $\delta U'$ , expressed as a percentage, can be estimated from Formula (3):

$$\delta U' = 25 \left| \frac{C_{D \text{ and } D/2}}{C_F} - 1 \right| \quad (3)$$

where  $C_{D \text{ and } D/2}$  is the discharge coefficient for  $D$  and  $D/2$  tapplings.

### 6.4.4 Example

Consider an orifice meter with  $\beta = 0,6$ ,  $Re_D = 10^6$ ,  $D = 250$  mm and tapplings at  $0,15D$  upstream and downstream of the plate.

To estimate the discharge coefficient, use ISO 5167-2:2022, Formula (4), with  $L_1 = L'_2 = 0,15$ .

The tapplings in this example lie between the flange tapping and  $D$  and  $D/2$  tapping positions. From, respectively, ISO 5167-2:2022, Tables A.8 and A.2:  $C_F = 0,605$  1;  $C_D$  and  $D/2 = 0,607$  0. Therefore

$$\delta U' = 25 \left| \frac{0,605}{0,607} - 1 \right| = 0,078$$

The relative expanded uncertainty in the discharge coefficient at  $k = 2$  (approximately 95 % confidence level) is 0,5 % (see ISO 5167-2:2022, 5.3.3.1).

Therefore, the overall relative expanded uncertainty at  $k = 2$  (approximately 95 % confidence level) is  $0,5 + 0,078 \approx 0,6$  % (i.e. the uncertainties have simply been added together).

## 6.5 Condition of pressure tapplings

Experience has shown that large errors can be created by pressure tapplings which have burrs or deposits on, or close to, the edge where the tapping penetrates the pipe wall. This is particularly the case where the tapplings are in the main flow stream, such as throat tapplings in nozzles or Venturi tubes, where small burrs can give rise to significant percentage errors. Upstream corner tapplings and downstream tapplings in relatively dead zones are much less liable to cause this problem.

The installation is inspected before use and at regular intervals to ensure that these anomalies are not present.

## 7 Effects of pipeline near the meter

### 7.1 Pipe diameter

The internal diameter of the pipe upstream and downstream of the primary device is always measured to ensure that it is in accordance with ISO 5167-2:2022, 6.4, ISO 5167-3:2022, 6.4 or ISO 5167-4:2022, 6.4.1. Errors in the upstream internal diameter measurement cause errors in the calculated flowrate, which are given by [Formula \(4\)](#):

$$\frac{\delta q_m}{q_m} = \frac{-2\beta^4}{(1-\beta^4)} \frac{\delta D}{D} \quad (4)$$

These errors become significant for large  $\beta$ , e.g. with  $\beta = 0,75$ , a positive 1 % error in  $D$  causes a negative 1 % error in  $q_m$ .

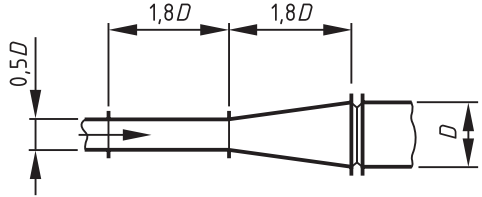
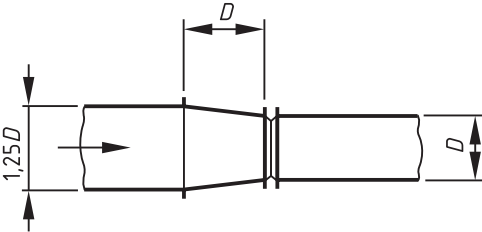
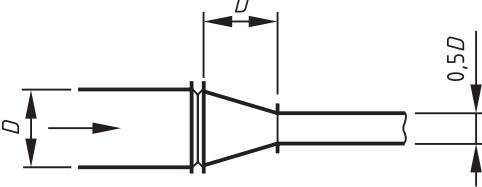
The downstream pipe is far less critical, as for an orifice plate, an ISA 1932 nozzle or a long radius nozzle its diameter need only be within 3 % of that of the upstream pipe (see ISO 5167-2:2022, 6.4.6 or ISO 5167-3:2022, 6.4.6) and for a Venturi nozzle or a Venturi tube its diameter need only be  $\geq 90$  % of the diameter at the end of the divergent section (see ISO 5167-3:2022 6.4.6 or ISO 5167-4:2022, 6.4.1.3).

### 7.2 Steps and taper sections

Sudden enlargements of the pipe in the vicinity of the primary device are always to be avoided as large errors in flow measurement result from their use. Similarly, tapering sections of pipe can lead to significant errors, as can be seen from [Table 2](#) which gives the order of errors to be expected when an orifice plate with corner tapplings is immediately preceded or followed by a taper piece.

The information in [Table 2](#) indicates that a taper piece divergent in the direction of flow, and placed immediately upstream, is not recommended, since discharge-coefficient increases of up to 50 % result. On the other hand, a convergent taper piece, whether installed before or after the orifice plate, and provided it is not of a steeper angle than those shown, results in coefficient changes of generally less than 2 %.

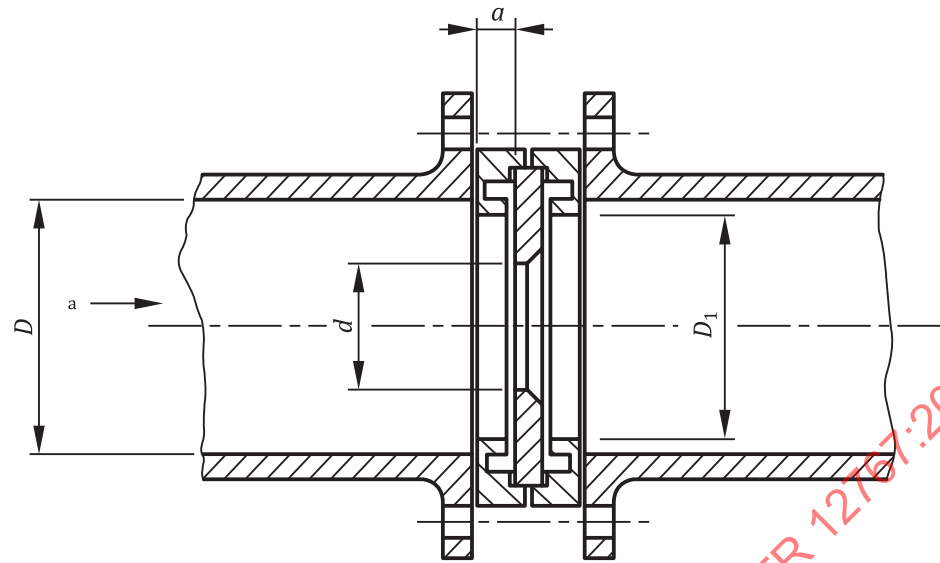
Table 2 — Effect of taper pieces

Position of orifice plate	$\beta$	Order of the discharge coefficient change to be expected %
a) Immediately downstream of a divergent taper piece 	0,4 0,7	+10 +50
b) Immediately downstream of a convergent taper piece 	0,4 0,7	-0,5 -2
c) Immediately upstream of a convergent taper piece 	0,4 0,7	0 to -1 +1

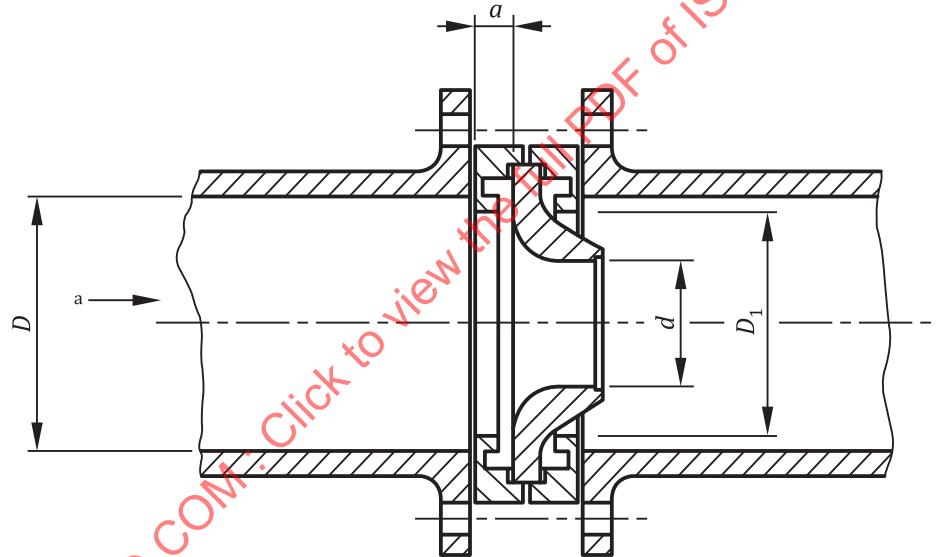
7.3 Diameter of carrier ring

The requirements for the sizing and concentric mounting of carrier rings for orifice plates and nozzles are specified in ISO 5167-2:2022, 6.4 and 6.5, ISO 5167-3:2022, 6.4 and 6.5 and ISO 5167-2:2022, Figure 4. If the requirement of ISO 5167-2:2022, 6.5.4 and ISO 5167-3:2022, 6.5.4 (i.e. that the centred carrier ring does not protrude into the pipe) is not met, relatively large flow-measurement errors are introduced. [Figure 3](#) shows such an installation and [Figure 4](#), using the same notation, shows the approximate errors introduced for the given conditions, where  $a$  is the width of the portion of the carrier ring upstream of the upstream face of the orifice plate or nozzle. It is emphasized that in arriving at these errors, the internal carrier ring diameter,  $D_1$ , and not the diameter of the main line, has been used in determining the calculated flowrate and is to be used for  $D$  in determining the correction factor when making use of the values shown.

Where the carrier is oversize, experimental results indicate that for  $\beta = 0,74$  a carrier 11 % oversize and extending  $0,05D$  upstream from the plate increased the discharge coefficient by approximately 0,5 %. However, for a similar geometry but with  $\beta = 0,63$ , no effect was found.



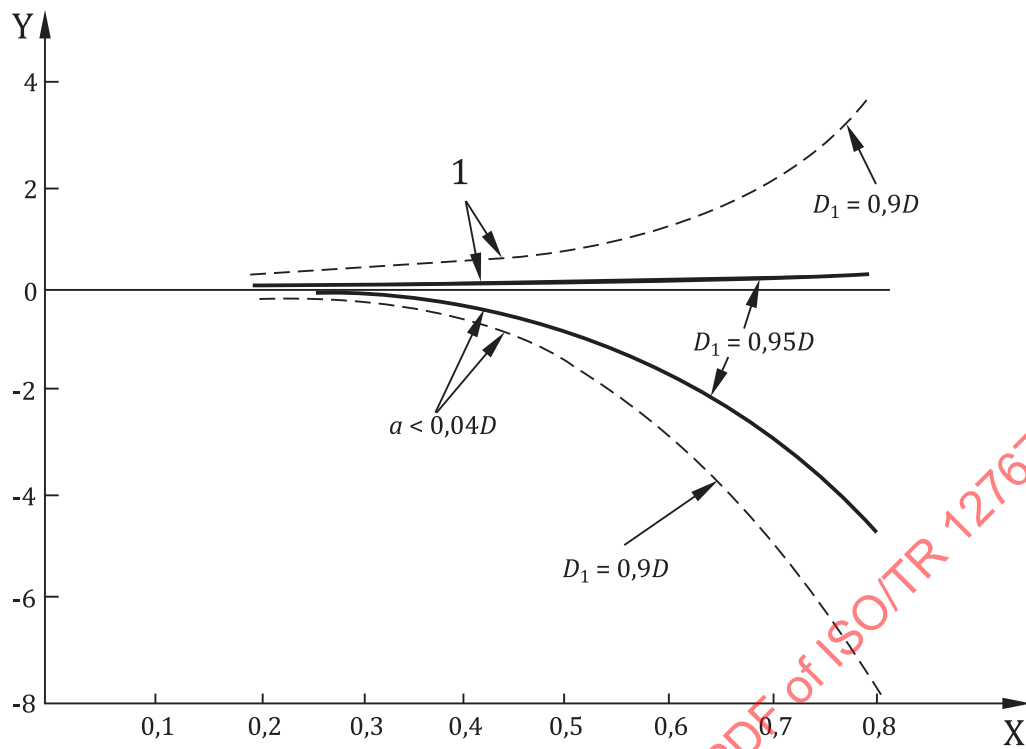
a) Orifice plate



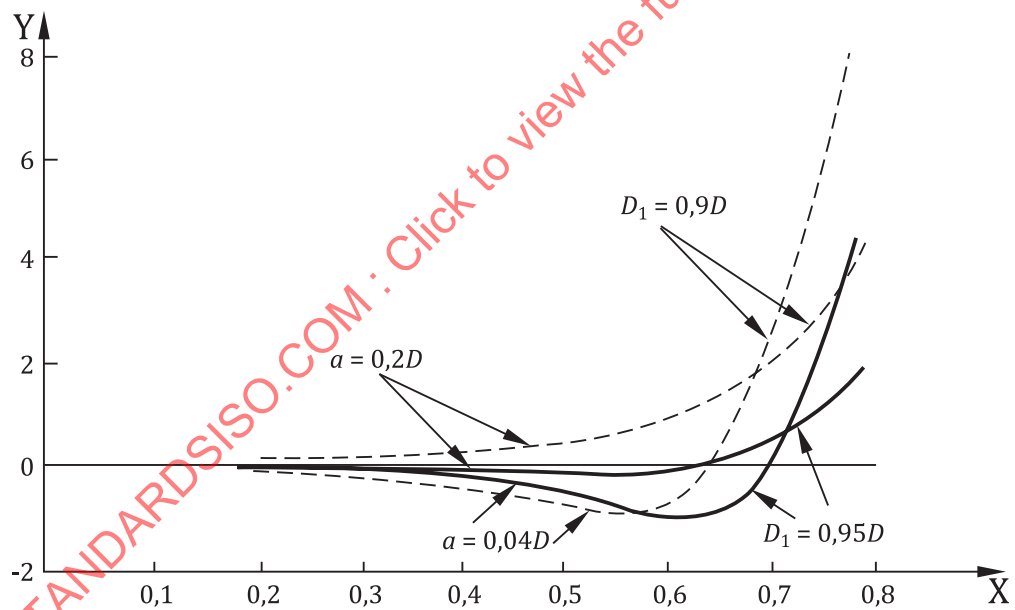
b) Nozzle

a Direction of flow.

**Figure 3 — Carrier having internal diameter,  $D_1$ , less than pipe diameter,  $D$**



a) Orifice plate



b) Nozzle

**Key**

X diameter ratio

Y change in discharge coefficient (%)

1  $a = 0,2D$  to  $0,3D$

**Figure 4 — Effect of incorrect carrier diameter**



## 7.4 Undersize joint rings

When the inside diameter of a joint ring or gasket is smaller than the pipe diameter, especially on the upstream side of an orifice plate or nozzle, very large flow-measurement errors might occur. The magnitude and sign of the effect in relation to the measurement of flowrate is dependent on the combination of a number of variables, e.g. the thickness of the joint ring upstream of the orifice plate, the extent of its protrusion into the flow, its position relative to the orifice plate and pressure tapings, and the degree of roughness of the upstream pipe.

## 7.5 Protruding welds

The effect of an undressed circumferential weld protruding into the pipe bore adjacent to the primary device is similar to that of an undersize joint ring. Such an effect might arise from the fitting of a weld-neck flange, and the magnitude of the effect depends on the height uniformity, or otherwise, of the protruding weld, and its position in relation to the single or multiple pressure tapping arrangement employed to measure the differential pressure across the primary device. To quantify the resulting error in a specific situation is difficult without a direct calibration.

Seamed pipe is acceptable, provided that the internal weld bead is parallel to the pipe axis throughout the entire length of the pipe required, to satisfy the installation requirements for the primary device being used, and any weld bead does not have a height greater than the permitted step in diameter. Unless an annular slot is used, the seam is not situated within any sector of  $\pm 30^\circ$  centred on any individual pressure tapping to be used in conjunction with the primary device. If an annular slot is used, the location of the seam is not significant. If spirally wound pipe is used, then it is machined to a smooth bore. (See ISO 5167-1:2022, 7.1.4.)

## 7.6 Eccentricity

The requirements for concentric mounting of the device are given in ISO 5167-2:2022, 6.5.3 and 6.5.4, ISO 5167-3:2022, 6.5.3 and 6.5.4 and ISO 5167-4:2022, 6.4.1. The geometric measure of eccentricity is the distance between the pipe and orifice plate centrelines and is often expressed as a percentage of the pipe diameter,  $D$ . [Figure 5](#) shows the eccentric mounting of an orifice plate in a sideways direction relative to the upstream pipeline. The displacement is to the right and the eccentricity is a combination of the dimensional tolerances arising from the bolt-hole pitch-circle diameter, the bolt diameter, the bolt-hole diameter and the outer diameter of the orifice plate.

Experimental evidence on the effects of eccentricity is limited, but it has been shown that for orifice plates, the effect on discharge coefficient is a function of  $\beta$ , pipe size and roughness, pressure-tapping type, location and magnitude, as well as the position of the orifice centre relative to the pressure tapping.

Experimental work indicates that the errors due to eccentricity increase in general with  $\beta$ . For  $\beta = 0,2$  and eccentricity up to 5 % of  $D$ , discharge coefficient increases are unlikely to exceed 0,1 %. For larger  $\beta$ , the changes are best shown graphically as in [Figure 6](#).

Below 3 % eccentricity, the error varies with type of tapings and direction of eccentricity. The meter is least sensitive to eccentricity perpendicular to the tapings. Above 3 % eccentricity, errors for all tapings and directions increase rapidly.

**NOTE** No data are available for corner tapings, but the errors are probably similar to those for flange tapings since the above data were obtained from a test line with  $D = 150$  mm.

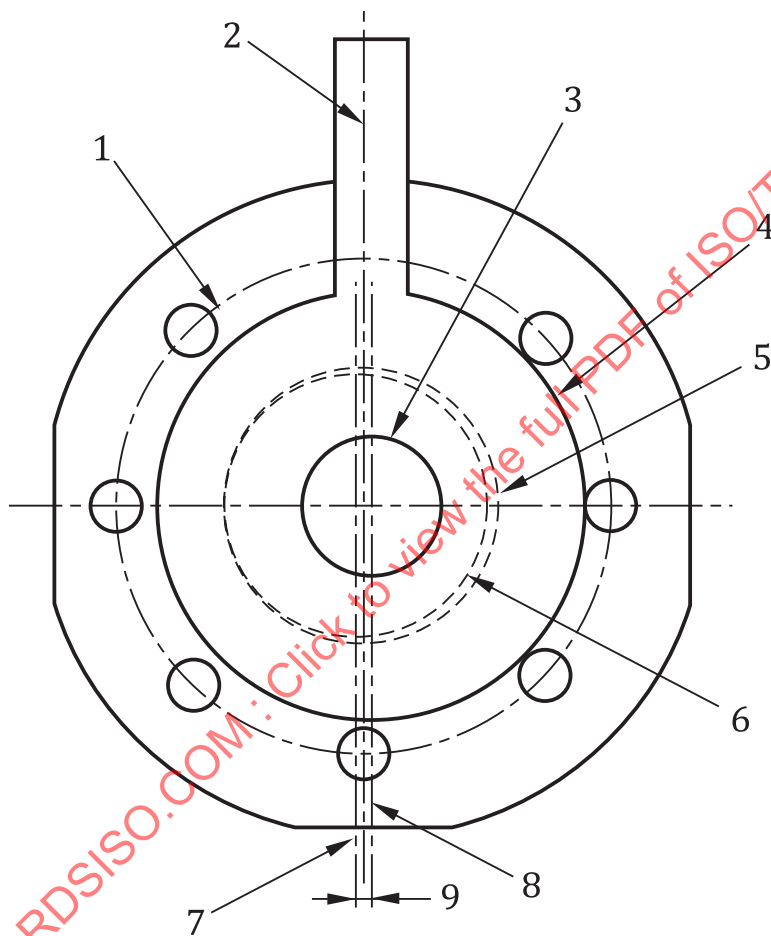
A further effect of eccentric positioning of an orifice plate is an increased unsteadiness of the differential pressure signal obtained. Observations have shown, for example, a marked increase in differential pressure reading fluctuations with increasing eccentricity for all values of  $\beta$  between 0,4 and 0,7.

Because of the number of variants contributing to the effect of eccentricity on the measurement of flow, the effect is difficult to quantify. It is very important to restrict eccentricity to less than 3 % of  $D$ , particularly in the direction of the tapings.

The effect of eccentricity is minimized by employing four equally-spaced upstream and downstream tapings on the flowmeter, as illustrated in ISO 5167-1:2022, Figure 1. The pressure lines from these are then coupled in the widely used triple-T tapping arrangement in order to obtain an average differential pressure reading.

As a general guide, a reasonable assumption is that the effects of eccentric mounting for multi-tapped nozzles will be less than those for orifice plates of equivalent  $\beta$ . Venturi tubes are less likely to be installed off-centre.

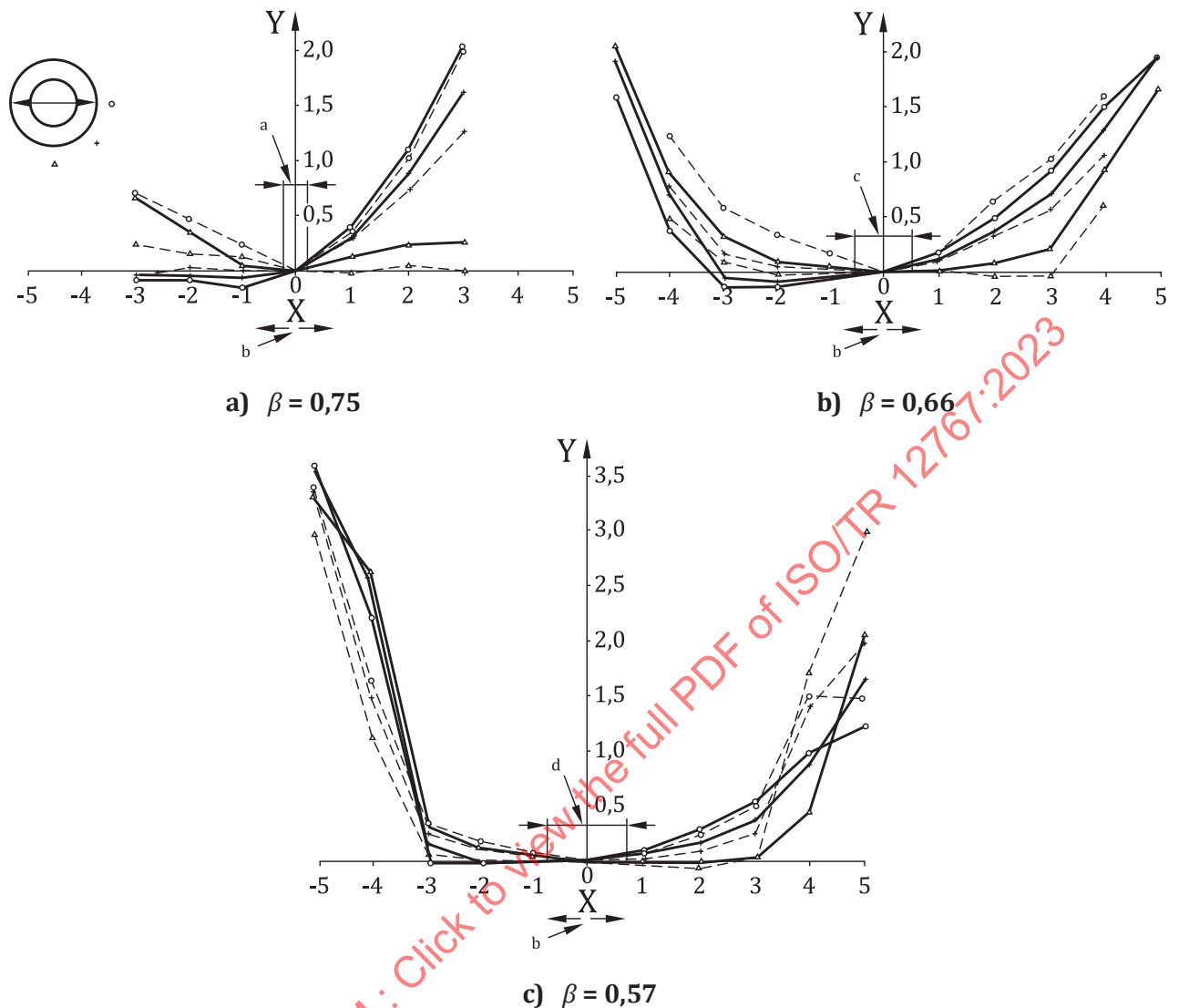
**NOTE** Combined installation faults: it is recommended that errors arising from the combined effects of eccentricity, carrier ring steps, etc., are not taken into account additively. The total possible error will be governed by the strongest of the effects present.



**Key**

- 1 bolt-hole pitch circle
- 2 flange centreline
- 3 orifice bore
- 4 orifice-plate outside diameter
- 5 flange bore
- 6 pipe inside diameter
- 7 pipe centreline
- 8 orifice centreline
- 9 eccentricity

**Figure 5 — Possible orifice-plate eccentricity resulting from specified tolerances on bolt hole, bolt hole pitch circle, pipe outside diameter and flange bore**

**Key**

- X eccentricity (%)
- Y change in discharge coefficient (%)
- $D$  and  $D/2$  tapplings
- - - flange tapplings
- a  $\pm 0,3$  %.
- b (away from tapping 1)  $\leftarrow \rightarrow$  (towards tapping 1).
- c  $\pm 0,5$  %.
- d  $\pm 0,7$  %.

**Figure 6 — Discharge coefficient error vs. eccentricity for an orifice plate with  $D$  and  $D/2$  and flange tapplings**

## 8 Effects of pipe layout

### 8.1 General

Minimum values of the straight lengths required between the primary device and various upstream fittings are given in ISO 5167-2:2022, 6.2, ISO 5167-3:2022, 6.2 and ISO 5167-4:2022, 6.2. Minimum

straight lengths are given both for “zero additional uncertainty” and for “0,5 % additional uncertainty” in the discharge coefficient.

When the minimum requirements for even “0,5 % additional uncertainty” cannot be satisfied, it is appropriate for the user both to make a correction to compensate for the change in the discharge coefficient and to increase the value of the percentage uncertainty.

Corrections and additional uncertainties for square-edged orifice plates with corner, flange and  $D$  and  $D/2$  tappings are given in [Tables 3](#) and [4](#) for a variety of upstream pipe bends and fittings. Shifts in columns 4 and 5 are particularly variable, depending on the exact details of the double bend.

Additional data on shifts in orifice-plate discharge coefficients for a large number of upstream fittings are given in References [\[8\]](#) to [\[11\]](#).

## 8.2 Discharge coefficient compensation

### 8.2.1 Corrections

The discharge coefficient can be corrected using the data in [Table 3](#) as illustrated in the following examples:

- a) percentage change in coefficient is +1,1 %, therefore the coefficient is multiplied by 1,011;
- b) percentage change in coefficient is -2,3 %, therefore the coefficient is multiplied by 0,977.

**Table 3 — Percentage change in discharge coefficient,  $c$ , when the straight pipe lengths before the orifice are less than those specified in ISO 5167-2**

Upstream straight length	$\beta$	Type of fitting (for details of nomenclature, see key)																
		1	2	3	4	5	6	7	8	9	10	11	12	13	14	15	16	17
4D	0,5	-1,4	-1,4	-0,5	+2,9	+2,9	-0,4	+8,2	—	+0,2	+0,2	-1,0	-0,8	+0,3	+0,5	+0,2	—	—
	0,6	-2,3	-2,2	-1,1	+1,7	+1,3	-1,2	+8,5	—	-0,2	-0,3	-2,4	-1,7	+0,3	0	-0,2	—	—
	0,7	-3,8	-3,2	-1,8	+0,1	+0,4	-2,1	+8,2	—	-0,9	-0,7	-4,4	-2,3	+0,3	-0,6	0	—	—
	0,8	-5,6	— <sup>b</sup>	-2,6	-2,4	— <sup>b</sup>	-3,1	+3,4	—	-2,2	— <sup>b</sup>	-7,5	— <sup>b</sup>	+0,3	-1,3	— <sup>b</sup>	—	—
8D	0,5	-0,7	-0,7	-0,3	+2,4	+2,4	0	+6,3	+6,4	-0,2	-0,2	-0,6	-0,4	— <sup>a</sup>	-0,2	-0,2	-0,8	-0,7
	0,6	-1,4	-1,2	-0,7	+1,4	+1,2	-0,7	+5,6	+6,1	-0,6	-0,4	-1,3	-1,2	— <sup>a</sup>	-0,7	-0,8	-1,3	-1,2
	0,7	-2,2	-1,9	-1,2	+0,3	+0,4	-1,3	+4,4	+6,1	-1,1	-0,8	-2,1	-1,9	+0,1	-1,2	-1,2	-1,7	-1,7
	0,8	-3,2	— <sup>b</sup>	-1,8	-1,7	— <sup>b</sup>	-2,0	+2,3	— <sup>b</sup>	-1,9	— <sup>b</sup>	-3,1	— <sup>b</sup>	+0,1	-1,8	— <sup>b</sup>	-2,0	-2,1
12D	0,5	— <sup>a</sup>	— <sup>a</sup>	— <sup>a</sup>	+2,0	+2,0	0	+5,5	+5,5	-0,2	-0,1	-0,4	-0,3	— <sup>a</sup>	-0,3	-0,2	—	— <sup>c</sup>
	0,6	-0,8	-0,8	-0,4	+1,2	+1,0	-0,4	+3,9	+4,3	-0,4	-0,3	-0,9	-0,9	— <sup>a</sup>	-0,7	-0,6	-0,8	-0,8 <sup>c</sup>
	0,7	-1,4	-1,4	-0,8	+0,3	+0,3	-0,8	+2,6	+3,2	-0,8	-0,7	-1,3	-1,3	— <sup>a</sup>	-1,1	-1,0	-1,2	-1,1
	0,8	-2,0	— <sup>b</sup>	-1,3	-1,3	— <sup>b</sup>	-1,3	+1,5	— <sup>b</sup>	-1,3	— <sup>b</sup>	-1,7	— <sup>b</sup>	—	-1,5	— <sup>b</sup>	-1,5	-1,4
16D	0,5	— <sup>a</sup>	— <sup>a</sup>	— <sup>a</sup>	+1,7	+1,7	0	+5,1	+5,0	-0,1	0	-0,2	-0,2	— <sup>a</sup>	-0,2	-0,2	—	—
	0,6	— <sup>a</sup>	— <sup>a</sup>	-0,3	+1,1	+0,9	-0,3	+3,5	+3,6	-0,3	-0,2	-0,6	-0,6	— <sup>a</sup>	-0,4	-0,4	—	—
	0,7	-0,8	-0,8	-0,5	+0,3	+0,3	-0,5	+2,1	+2,4	-0,5	-0,5	-0,9	-1,0	— <sup>a</sup>	-0,7	-0,6	-0,9	—
	0,8	-1,3	— <sup>b</sup>	-0,7	-1,1	— <sup>b</sup>	-0,8	+0,8	— <sup>b</sup>	-0,8	— <sup>b</sup>	-1,0	— <sup>b</sup>	—	-1,0	— <sup>b</sup>	-1,2	—

<sup>a</sup> Refer to ISO 5167-2:2022, Table 3.

<sup>b</sup> For  $D$  and  $D/2$  tappings, discharge coefficient changes measured for  $\beta > 0,75$  are not used for interpolation to give discharge coefficient changes for  $\beta \leq 0,75$ , as the downstream tapping is in the pressure recovery region if  $L_2' > 2(1 - \beta)$ .

<sup>c</sup> For a concentric expander 0,5D to  $D$  over a length of  $D$  to  $2D$  refer to ISO 5167-2:2022, Table 3.

Key					
No.	Type of upstream fitting	Type of tappings	No.	Type of upstream fitting	Type of tappings
1	Single short radius 90° bend	C o r n e r , flange	10	Butterfly valve, fully open	$D$ and $D/2$
2	Single short radius 90° bend	$D$ and $D/2$	11	Butterfly valve, 52° open	C o r n e r , flange
3	Two 90° bends in the same plane, U- or S-configuration, $0D$ to $10D$ spacer	All	12	Butterfly valve, 52° open	$D$ and $D/2$
4	Two 90° bends at right angles, no spacer	C o r n e r , flange	13	Gate valve, fully open	All
5	Two 90° bends at right angles, no spacer	$D$ and $D/2$	14	Gate valve, $\frac{2}{3}$ open	C o r n e r , flange
6	Two 90° bends at right angles, $5D$ to $11D$ spacer	All	15	Gate valve, $\frac{2}{3}$ open	$D$ and $D/2$
7	Two 90° mitre bends at right angles, no spacer	C o r n e r , flange	16	Gate valve, $\frac{1}{4}$ open and globe valve	All
8	Two 90° mitre bends at right angles, no spacer	$D$ and $D/2$	17	Symmetrical enlargement, tapered or abrupt	All
9	Butterfly valve, fully open	C o r n e r , flange			

**Table 4 — Formulae for additional uncertainty in the orifice discharge coefficient, to be used with the percentage changes given in Table 3, for all tapping arrangements**

Type of upstream fitting	Formulae for additional percentage relative expanded uncertainty	
	Piezometer ring e.g. Triple-T	Single tapping <sup>a</sup>
Single short radius 90° bend. Bend radii $1D$ to $1,5D$	$0,5(1 + 0,6 c )$	$0,5 + 0,6 c $
Two 90° bends, U- or S-configuration, in same plane	$0,5(1 +  c )$	$0,5 +  c $
Two 90° bends at right angles, no spacer (where $X$ is the distance from the orifice plate to the nearest bend)	$0,5(1 +  c ) + (10D/X)$	$0,5 +  c  + (10D/X)$
Two 90° bends at right angles, $5D$ to $11D$ spacer	$0,5 +  c $	$0,5(1 + 3 c )$
Two 90° mitre bends at right angles, no spacer	$0,5 +  c $	$0,5(1 + 3 c )$
Butterfly valve, fully open	$0,5 +  c $	$0,5(1 + 3 c )$
Butterfly valve, 52° open	$0,5 +  c $	$0,5(1 + 3 c )$
Gate valve, fully open	$0,5(1 +  c )$	$0,5 +  c $
Gate valve, $\frac{2}{3}$ open	$0,5(1 +  c )$	$0,5 +  c $
Gate valve, $\frac{1}{4}$ open and globe valve	$0,5 +  c $	$0,5 +  c $
Symmetrical restriction or enlargement, tapered or abrupt	$0,5 +  c $	$0,5 +  c $

<sup>a</sup> The tapping axis is at right angles to the plane of the nearest upstream bend.

## 8.2.2 Additional uncertainty

The formulae for calculating the additional percentage relative expanded uncertainty in the discharge coefficient are given in Table 4 for each type of fitting. This is in addition to the basic relative expanded uncertainty in the discharge coefficient of: 0,5 % for  $0,2 \leq \beta \leq 0,6$ ,  $(1,667\beta - 0,5)$  % for  $0,6 < \beta \leq 0,75$ . In

deriving the formulae, the quantity of data, its consistency and corroboration from different sources have been taken into account. Their use is illustrated in the following examples.

- a) If the formula to be applied is [Formula \(5\)](#):

$$\delta U' = 0,5(1 + |c|) \quad (5)$$

where  $|c|$  is the modulus of percentage change (i.e. the magnitude irrespective of sign) and if the change in the coefficient is +1,4 %, then  $\delta U' = 1,2$  %.

- b) If the formula to be applied is [Formula \(6\)](#):

$$\delta U' = 0,5 + |c| \quad (6)$$

and if  $c = -2,8$  %, then  $\delta U' = 3,3$  %.

### 8.3 Pressure tapplings

It is emphasized that the change in the coefficient when  $D$  and  $D/2$  tapplings are used is often different from those obtained with corner or flange tapplings.

When the upstream straight pipe length is less than that required for “zero additional uncertainty”, it is best that multiple tapplings with triple-T connections, as shown in ISO 5167-1:2022, Figure 1 are used and that if single tapplings are used, their axes are at right angles to the plane of the nearest upstream bend.

### 8.4 Devices for improving flow conditions

Flow conditioners are used where asymmetric or swirling flow has to be measured. Descriptions of various flow conditioners are provided in ISO 5167-2:2022 [6.3 or Annex B]. Even where the installation requirements of ISO 5167-2:2022 [6.3 or Annex B] cannot be met, the use of a flow conditioner might reduce errors especially in swirling flow.

## 9 Operational deviations

### 9.1 General

Metering systems that conform to ISO 5167 when new or recently maintained might be subject to a significant degradation in accuracy over the passage of time.

This degradation might result from several causes:

- a) deformation of the orifice plate;
- b) deposition on the upstream face of an orifice plate;
- c) deposition in the meter tube;
- d) rounding of the orifice-plate edge;
- e) deposition in the pressure tapplings;
- f) deposition and increase of surface roughness in a Venturi tube.

An indication of the effect of sources of error a) to d) and f) is given in [9.2](#) to [9.6](#).

It cannot be emphasized too strongly that the continued achievement of high accuracy requires the expenditure of considerable effort. In particular, regular inspection and maintenance are essential.

Inspection periods depend on the nature of the fluid being metered and on the manner of operation of the system in which the meter is installed, and can only be determined from experience.

## 9.2 Deformation of an orifice plate

### 9.2.1 General

An orifice plate might be said to be deformed when it deviates beyond the 0,5 % value specified in ISO 5167-2:2022, 5.1.3.1. The deformation might be in the upstream or downstream direction, and possible causes are defects in manufacture, poor installation or incorrect use. It is important to rectify manufacturing and installation faults before use.

Deformation arising from the manner of use is either temporary (elastic) or permanent (buckling). This is discussed in References [12] to [14]. Information regarding the necessary thickness of orifice plates when metering systems are being designed is given in ISO/TR 9464:2023[4], 5.2.5.1.2.3.

### 9.2.2 Elastic deformation

Elastic deformation arises when the differential pressure due to flow deforms the plate by a small amount in the downstream direction, such that the induced stresses remain within the elastic limit of the plate material. For a plate simply supported at its rim, a first approximation to the percentage increase in discharge coefficient is given by [Formula \(7\)](#):

$$c = \frac{\Delta p}{Y} \left( \frac{D_2}{E} \right)^2 \left( \frac{a D_2}{E} - b \right) \quad (7)$$

where

$$a = \beta (13,5 - 15,5 \beta)$$

$$b = 117 - 106 \beta^{1,3}$$

For ASTM/AISI grades 304 or 316 stainless steel (ISO 15510[5]),  $Y$  can be taken as  $193 \times 10^9$  Pa.

In virtually all cases, the result of the deformation is to cause an increase in the discharge coefficient.

Errors due to elastic bending might be additional to those arising from initial lack of flatness. Only when the combination of both effects results in a slope greater than 1 % under flowing conditions does the plate depart from the requirements of ISO 5167-2.

Since the plate will return to its undeformed state when the flow is zero, elastic bending cannot be detected during routine inspection of a metering system.

### 9.2.3 Plastic deformation

Where an orifice plate has been subjected to excessive differential pressures it might deform permanently. When the deformation is known, it is possible to estimate the error from [Figure 7](#). Such deformation might occur during over-rapid pressurization or venting of a line containing a compressible fluid, or through an abnormal flow condition. Discard a permanently deformed plate.

The differential pressure required to reach orifice-plate yield stress,  $\Delta p_y$ , is estimated from [Formula \(8\)](#):

$$\Delta p_y = \sigma_y \left( \frac{E}{D_2} \right)^2 \left( \frac{1}{0,681 - 0,651 \beta} \right) \quad (8)$$



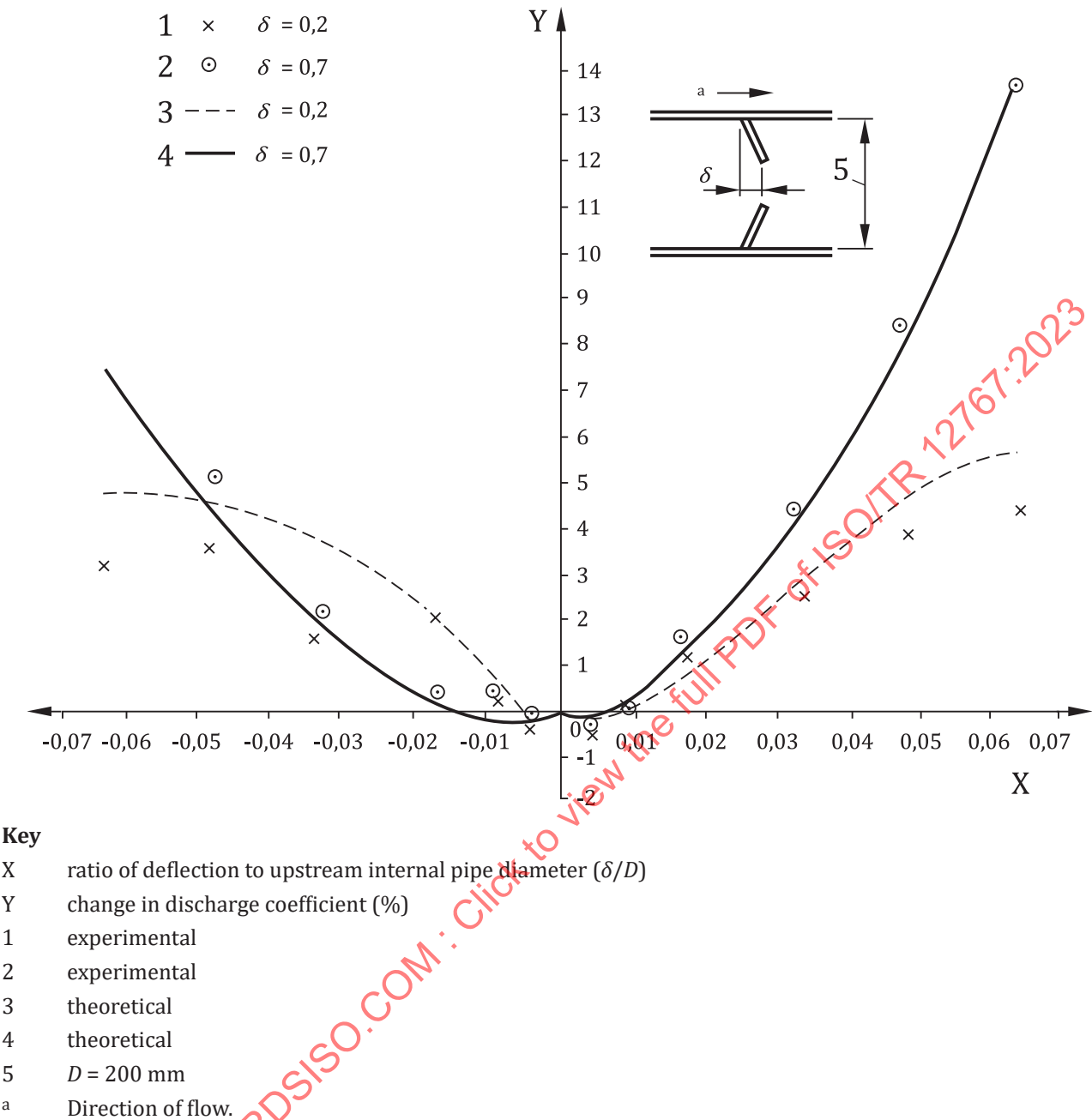


Figure 7 — Effect of orifice-plate deformation on flow-measurement accuracy

9.3 Deposition on the upstream face of an orifice plate

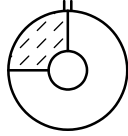


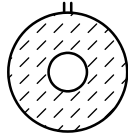
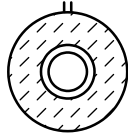
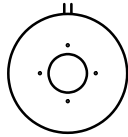
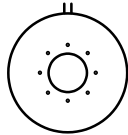
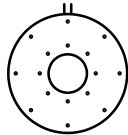
The effect of deposits on the upstream face of an orifice plate is similar to that of upstream face roughness and always causes the discharge coefficient to increase.

Table 5 shows the effect of a uniform layer of sand one grain thick (grain size 0,4 mm) and the effect of grease spots (each nominally 6,3 mm diameter and 2,5 mm high) on an orifice plate in a 100 mm diameter meter tube measuring air at atmospheric pressure. Table 5 shows the importance of the annular region around the entrance to the orifice bore. As this region is usually scrubbed by the flow, the actual errors are probably smaller than those indicated.



Table 6 shows the effect of a layer of Audco<sup>1)</sup> grease on an orifice plate of thickness 6 mm and of diameter ratio 0,6 in a 300 mm pipe. The pressure tapings were in the horizontal plane on the left of the drawings. The pipe Reynolds number was approximately  $10^7$ . For the tests, the orifice plate was removed from the carrier and moved into a laboratory area where contamination was added with the plate in a horizontal position. The contamination level given in Table 6 is that applied in the laboratory. The plate was then moved to a vertical position to allow any liquid to drain off before being reinserted into the carrier in the test line. During the subsequent 2 h test over a range of flowrates, the maximum increase in discharge coefficient (around the beginning of the test) and the saturation increase in discharge coefficient once the increase had become constant were recorded. Further information on the effect of contamination is given in References [15],[16].

**Table 5 — Effect of deposits on  $\beta = 0,2$  and  $\beta = 0,7$  orifice plates**

Deposit			Change in discharge coefficient, $c$	
			$\beta = 0,2$	$\beta = 0,7$
			%	
Sand	1 sand quadrant		+1,0	+0,8
	2 sand quadrants		+2,8	+1,9
	3 sand quadrants		+3,9	+2,4
	4 sand quadrants		+6,2	+ 3,0
	4 sand quadrants with 6 mm ring removed from around orifice bore		+0,3	+0,3
Grease	4 grease deposits		+1,0	+0,1
	8 grease deposits		+2,8	+1,3
	16 grease deposits		+2,1	+1,2

1) Example of a product available commercially. This information is given for the convenience of users of this document and does not constitute an endorsement by ISO of this product.

Table 5 (continued)

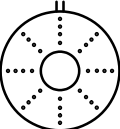
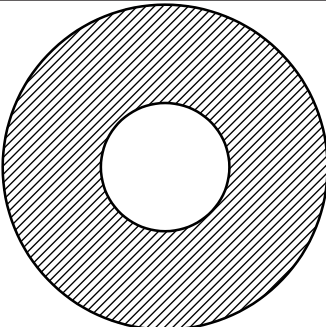
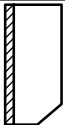
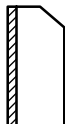
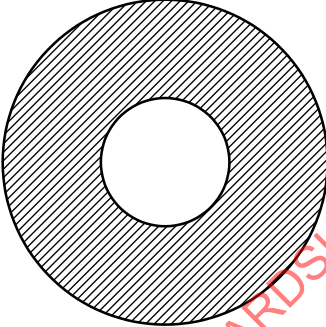


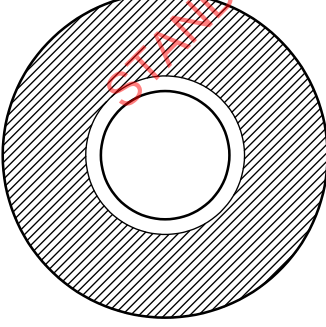
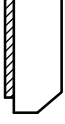
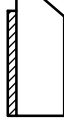
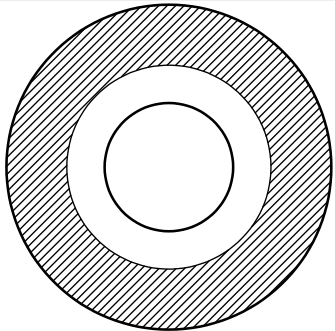
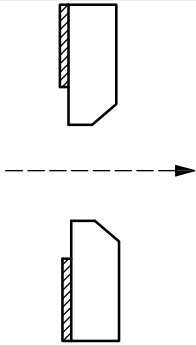
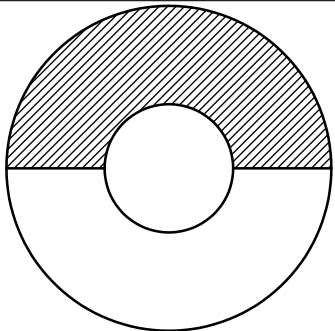
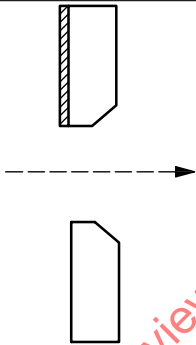
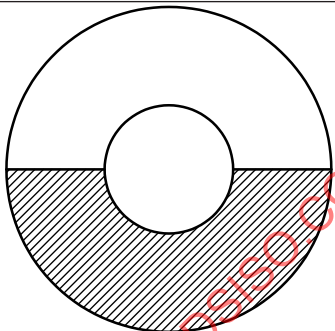
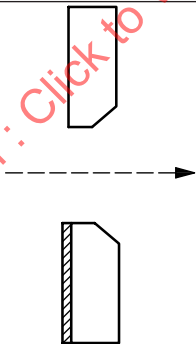
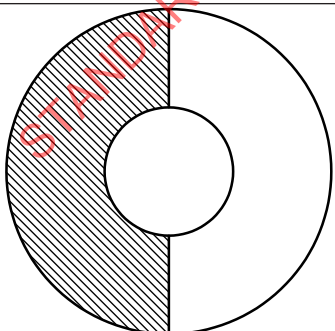
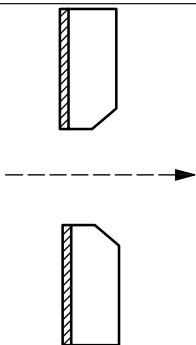
Deposit		Change in discharge coefficient, $c$	
		$\beta = 0,2$	$\beta = 0,7$
		%	
32 grease deposits		+2,6	+0,6

Table 6 — Increase in discharge coefficient,  $c$ , of an orifice plate,  $D = 300$  mm,  $\beta = 0,6$ , due to Audco<sup>a</sup> grease coating

Upstream face profile	Cross-section profile	Contaminant pattern	Maximum increase in discharge coefficient, $c$ %	Saturation increase in discharge coefficient, $c$ %	Coating thickness mm
	 -----> 	Full upstream face	2,85 3,49 5,15	2,15 2,13 3,70	0,6 1,2 2,0
	 -----> 	Full upstream face tapered off towards centre	1,30	1,00	1,2 to 0,0
	 -----> 	Full upstream face with 10 mm clean ring at centre	1,00	0,61	1,2

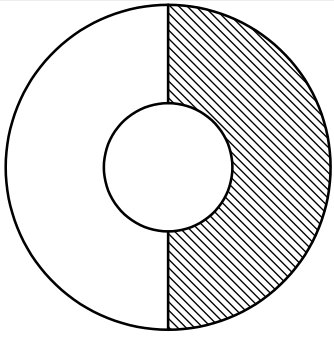
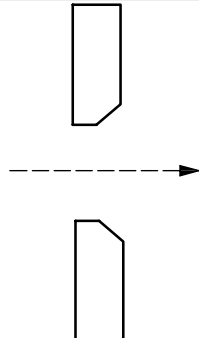
<sup>a</sup> Example of a product available commercially. This information is given for the convenience of users of this document and does not constitute an endorsement by ISO of this product.

Table 6 (continued)

Upstream face profile	Cross-section profile	Contaminant pattern	Maximum increase in discharge coefficient, $c$ %	Saturation increase in discharge coefficient, $c$ %	Coating thickness mm
		Full upstream face with 20 mm clean ring at centre	0,60	0,50	1,2
		Half circle at top of upstream face	1,70	—	1,2
		Half circle at bottom of upstream face	1,80	1,30	1,2
		Half circle vertical near tappings	2,20	0,85	1,2

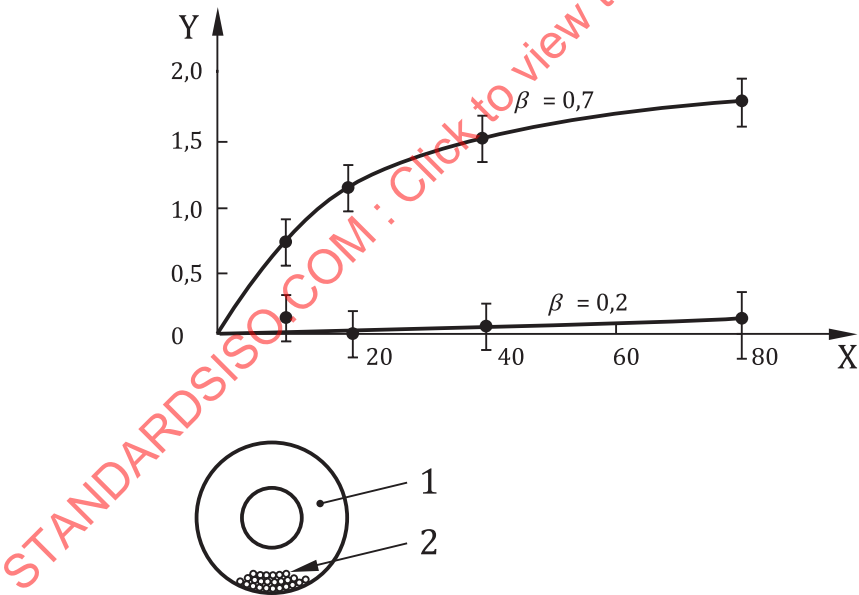
<sup>a</sup> Example of a product available commercially. This information is given for the convenience of users of this document and does not constitute an endorsement by ISO of this product.

Table 6 (continued)

Upstream face profile	Cross-section profile	Contami- nant pat- tern	Maximum increase in discharge coefficient, <i>c</i> %	Saturation increase in discharge coefficient, <i>c</i> %	Coating thickness  mm
		Half circle vertical away from tappings	3,70	2,84	1,2
<sup>a</sup> Example of a product available commercially. This information is given for the convenience of users of this document and does not constitute an endorsement by ISO of this product.					

9.4 Deposition in the meter tube

In an exercise to simulate the effect of deposition in the meter tube, welding rods were stacked axially against the upstream face of an orifice plate as shown in [Figure 8](#). The rods caused an increase in the discharge coefficient.



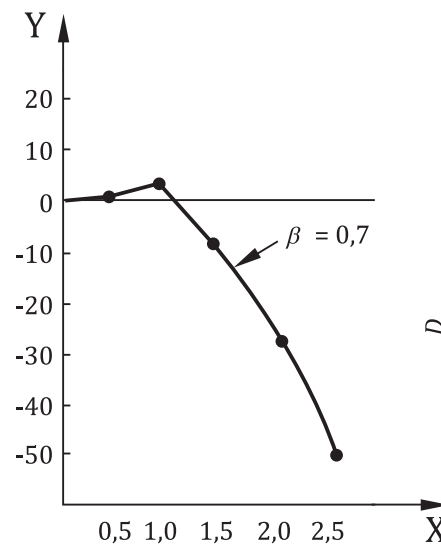
Key

- X number of welding rods
- Y change in discharge coefficient (%)
- 1 orifice plate
- 2 welding rods laid axially against orifice plate (rod diameter = 0,016*D*, rod length = 0,5*D*)

Figure 8 — Effect of welding rods in meter tube

[Figure 9](#) shows the results of tests carried out to investigate the effect of a smooth horizontal build-up of material in a meter run. When the material is below the dam height, the discharge coefficient

increases. When the build-up exceeds the dam height, the orifice bore cross-sectional area is reduced, leading to a decrease in discharge coefficient.



#### Key

- X obstruction level — fraction of dam height ( $2l/(D-d)$ )  
 Y change in discharge coefficient (%)  
 1 fraction of dam height

**Figure 9 — Effect of debris in meter tube (on both sides of plate)**

## 9.5 Orifice-plate edge sharpness

### 9.5.1 Deterioration

The sharp edge of an orifice plate might deteriorate with time. Possible causes of this deterioration are:

- erosion;
- cavitation;
- mechanical damage;
- careless handling.

Orifice-plate discharge coefficients are sensitive to edge sharpness, and, where any of the above effects might occur, it is advised that regular quantitative inspection of the edge is performed.

The effect of loss of sharp edge is described in [6.1](#).

### 9.5.2 Plate reversal

It is most important to ensure that bevelled orifice plates are inserted into the meter line with the bevel on the downstream face.

In a 100 mm diameter meter, a plate bevelled at  $45^\circ$  and facing upstream can give the following percentage increases in discharge coefficient:

- 0,25 mm bevel width:  $c = 2,0$ ;
- 0,5 mm bevel width:  $c = 4,0$ ;

c) 1,25 mm bevel width:  $c = 13,0$ .

These values are simply indicative of changes which can occur by incorrect installation and are not precise. Additional data are shown in Reference [62].

## 9.6 Deposition and increase of surface roughness in Venturi tubes

### 9.6.1 General

Two effects might occur in a Venturi tube which has been in use for a period of time. These are deposition of material in the contraction and the bore, and an increase in the surface roughness. Both effects result in a decrease in the discharge coefficient and both effects might occur together. They are, however, considered separately in 9.6.2 and 9.6.3.

### 9.6.2 Deposition

If material is deposited smoothly and uniformly in the contraction and bore of a Venturi tube, the change in discharge coefficient, expressed as a percentage,  $c$ , is estimated theoretically from the reduction in area as Formula (9):

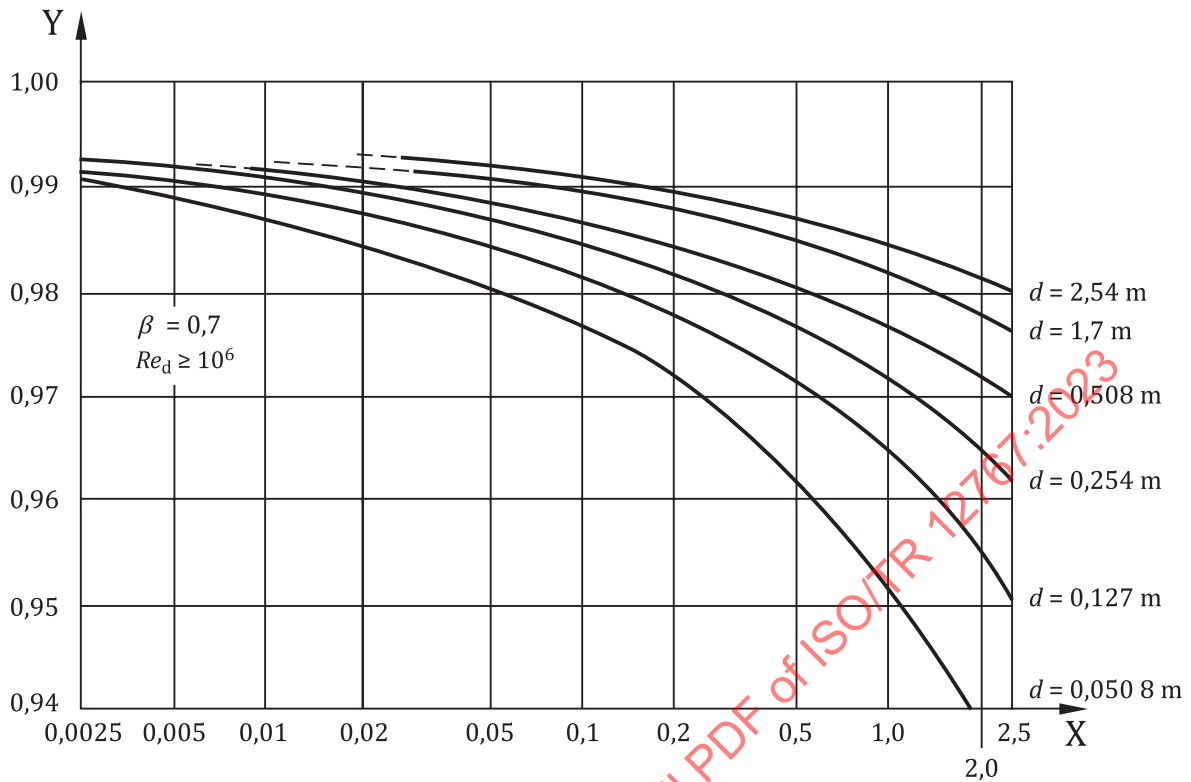
$$c = -400(l/d) \quad (9)$$

where  $l$  is the thickness, in metres, of the annular deposit in the bore of the Venturi tube.

### 9.6.3 Surface roughness

The chemical nature of the fluid and the material of the Venturi tube might be such that the surface roughness of the Venturi tube increases with time (Reference [17]). This increase in roughness leads to a reduction in the discharge coefficient. An indication of the error involved is given in Figure 10.

The rate of increase of surface roughness is dependent on the chemical reactions occurring in the metering system, and is outside the scope of this document.

**Key**

- X uniform equivalent roughness of Venturi tube ( $k$ ), mm  
Y Venturi tube discharge coefficient

**Figure 10 — Variation of Venturi meter coefficient with surface roughness**

## 10 Pipe roughness

### 10.1 General

The discharge coefficients given in ISO 5167-2:2022, 5.3.2.1, ISO 5167-3:2022, 5.1.6.2, 5.2.6.2 and 5.3.4.2 and ISO 5167-4:2022, 5.5 assume conformity to specified installation conditions. In particular, they are based on the assumption that the velocity profile immediately upstream of a primary device is similar to that in the experiments on which the equation is based.

The uniform equivalent pipe roughness,  $k$ , Reynolds number,  $Re_D$ , and friction factor,  $\lambda$ , are interrelated and determine the velocity profile (see Reference [18]). Experimental results suggest that the velocity profile, defined as the ratio of the local axial velocity at  $y$  from the pipe wall,  $u$ , to the velocity at the centreline ( $y/R = 1$ ),  $u_{CL}$ , can be described approximately by [Formula \(10\)](#):

$$\frac{u}{u_{CL}} = \left( \frac{y}{R} \right)^{1/n} \quad (10)$$

where

$y$  is the distance from the pipe wall;

$R$  is the pipe radius,  $D/2$ ;

$n$  is a number whose reciprocal gives the power (dependent on  $Re_D$  and  $k/D$ ) to which  $y/R$  must be raised to give the velocity profile.

The ratio of the mean axial velocity,  $U$ , to the velocity at the centreline ( $y/R = 1$ ),  $u_{CL}$ , is then given by [Formula \(11\)](#):

$$\frac{U}{u_{CL}} = \frac{2n^2}{(n+1)(2n+1)} \quad (11)$$

In smooth pipe,  $n$  increases with the Reynolds number (see [Table 7](#)). In fully rough pipe,  $n$  decreases with increasing relative roughness (see [Table 8](#)).

A more uniform profile ( $U/u_{CL} \rightarrow 1$ ) reduces the discharge coefficient and a more peaked profile ( $U/u_{CL}$  decreasing) increases  $C$ .

The extent to which the discharge coefficient varies is also influenced by  $\beta$ , being less for smaller  $\beta$ .

**Table 7 — Values of  $n$ ,  $U/u_{CL}$  and  $\lambda$  for smooth pipe**

$Re_D$	$n$	$U/u_{CL}$	$\lambda$
$4 \times 10^3$	6,0	0,791	0,04
$2,3 \times 10^4$	6,6	0,807	0,025
$1,1 \times 10^5$	7,0	0,817	0,017 5
$1,1 \times 10^6$	8,8	0,850	0,011 5
$2 \times 10^6$	10	0,866	0,010 5

**Table 8 — Values of  $n$ ,  $U/u_{CL}$  and  $\lambda$  for rough pipe**

$R/k$	$k/D$	$n$	$U/u_{CL}$	$\lambda$
507	$0,986 \times 10^{-3}$	6	0,791	0,020
126	$3,97 \times 10^{-3}$	5	0,758	0,028
31	$16,1 \times 10^{-3}$	4	0,711	0,045

## 10.2 Upstream pipe

For an orifice plate the change in discharge coefficient,  $\Delta C$ , due to pipe roughness is approximately proportional both to the change in friction factor,  $\Delta \lambda$ , and to  $\beta^{3,5}$ . The friction factor,  $\lambda$ , can be measured directly, using [Formula \(12\)](#):

$$\lambda = \frac{2D\Delta p}{\rho U^2 Z} \quad (12)$$

where

$D$  is the pipe diameter, in metres;

$\Delta p$  is the pressure difference, in pascals, between two tappings;

$\rho$  is the fluid density, in kilograms per cubic metre;

$U$  is the mean axial velocity, in metres per second;

$Z$  is the distance, in metres, between two tappings.



It is simpler to measure the arithmetic mean deviation of the roughness profile,  $R_a$ , to deduce the uniform equivalent roughness,  $k \approx \pi R_a$ , and to calculate  $\lambda$  using the Colebrook-White equation (see ISO 5167-1:2022, 7.4.1.5 and Equation (20.35a) of Reference [18]) given by [Formula \(13\)](#):

$$\frac{1}{\sqrt{\lambda}} = 1,74 - 2 \lg \left( \frac{2k}{D} + \frac{18,7}{Re_D \sqrt{\lambda}} \right) \quad (13)$$

If an estimate of the shift in discharge coefficient from ISO 5167-2:2022, Formula (4) is desired, it is also necessary to estimate the friction factor for the discharge coefficient equation. This has to be done on the basis of the measured roughness or friction factor of the pipes in which the standard data (to which the discharge coefficient equation was fitted) were collected; these are given in [Table 9](#). Both  $k/D$  and  $\lambda$  depend on  $Re_D$ ;  $k/D$  reduces with  $Re_D$  because the higher Reynolds numbers generally occur in larger pipes, which are generally relatively smoother.

**Table 9 — Values of  $k/D$  and  $\lambda$  associated with ISO 5167-2:2022, Formula (4)**

Pipe Reynolds No. $Re_D$	$10^4$	$3 \times 10^4$	$10^5$	$3 \times 10^5$	$10^6$	$3 \times 10^6$	$10^7$	$3 \times 10^7$	$10^8$
Ratio of uniform equivalent roughness to pipe diameter $k/D \times 10^4$	1,75	1,45	1,15	0,9	0,7	0,55	0,45	0,35	0,25
Friction factor $\lambda$	0,031	0,024	0,018 5	0,015 5	0,013	0,011 5	0,010 5	0,010	0,009 5

[Figure 11](#) gives measured and computed (using computational fluid dynamics) values of  $\Delta C$  as a function of  $\beta^{3,5} \Delta \lambda$  (see Reference [19] for complete references). The computed values and the European experimental data were obtained using corner tapplings. The North American experimental data (References [20] to [22]) were obtained using flange tapplings. For corner tapplings, the following approximate [Formula \(14\)](#) to calculate the change in discharge coefficient,  $\Delta C$ , has been plotted:

$$\Delta C = 3,5 \beta^{3,5} \Delta \lambda \quad (14)$$